Volume 19 | Number 9 | 7 March 2017 | Pages 6295–6890

PCCP

Physical Chemistry Chemical Physics

rsc.li/pccp

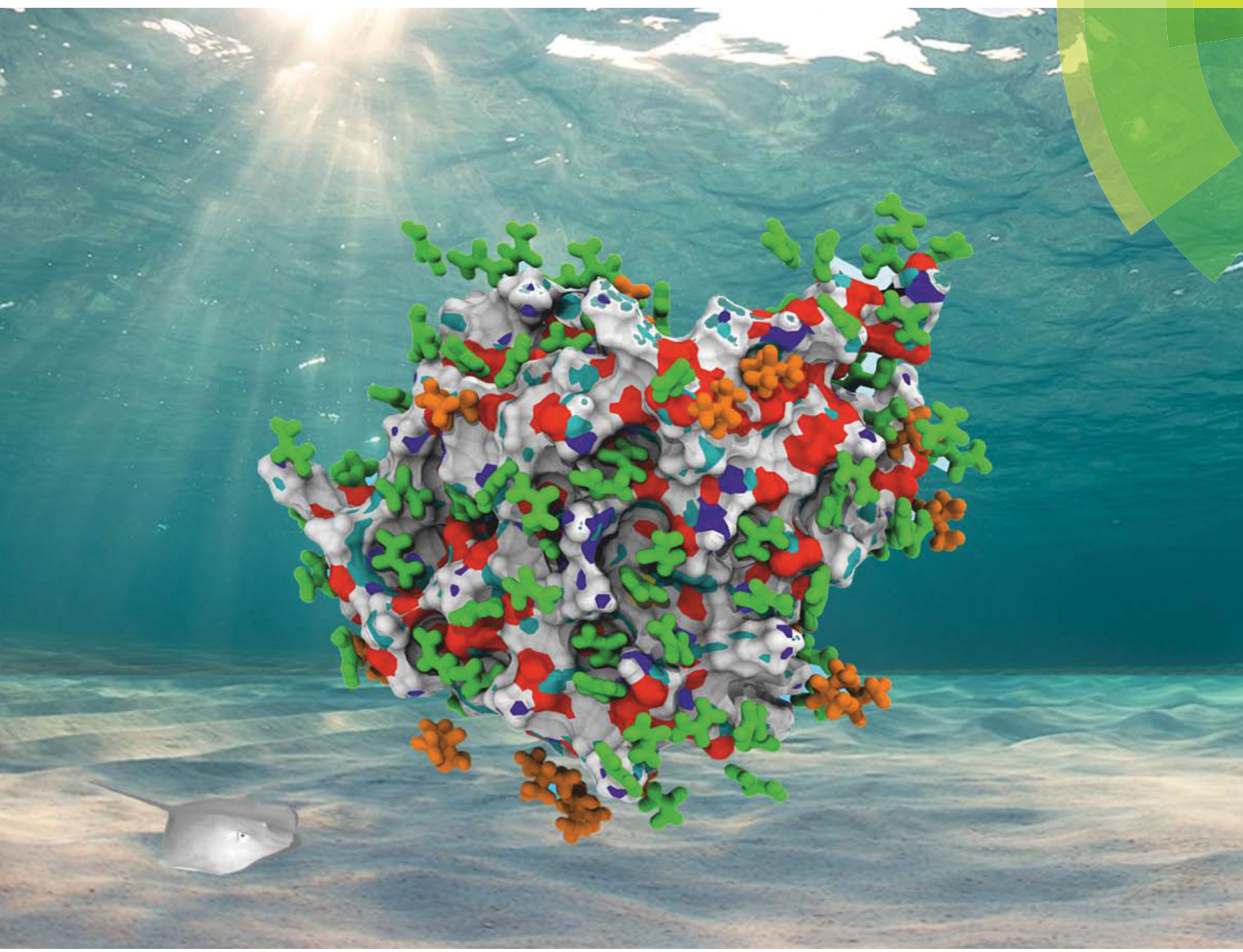

ISSN 1463-9076

ROYAL SOCIETY OF CHEMISTRY

PAPER

Roland Winter, Nikolai N. Medvedev *et al.*

TMAO and urea in the hydration shell of the protein SNase

PCCP

PAPER

View Article Online
View Journal | View Issue

Cite this: *Phys. Chem. Chem. Phys.*, 2017, **19**, 6345

TMAO and urea in the hydration shell of the protein SNase

Nikolai Smolin,[a] Vladimir P. Voloshin,[b] Alexey V. Anikeenko,[bc] Alfons Geiger,[d] Roland Winter*[d] and Nikolai N. Medvedev*[bc]

We performed all-atom MD simulations of the protein SNase in aqueous solution and in the presence of two major osmolytes, trimethylamine-*N*-oxide (TMAO) and urea, as cosolvents at various concentrations and compositions and at different pressures and temperatures. The distributions of the cosolvent molecules and their orientation in the surroundings of the protein were analyzed in great detail. The distribution of urea is largely conserved near the protein. It varies little with pressure and temperature, and does practically not depend on the addition of TMAO. The slight decrease with temperature of the number of urea molecules that are in contact with the SNase molecule is consistent with the view that the interaction of the protein with urea is mainly of enthalpic nature. Most of the TMAO molecules tend to be oriented to the protein by its methyl groups, a small amount of these molecules contact the protein by its oxygen, forming hydrogen bonds with the protein, only. Unlike urea, the fraction of TMAO in the hydration shell of SNase slightly increases with temperature (a signature of a prevailing hydrophobic interaction between TMAO and SNase), and decreases significantly upon the addition of urea. This behavior reflects the diverse nature of the interaction of the two osmolytes with the protein. Using the Voronoi volume of the atoms of the solvent molecules (water, urea, TMAO), we compared the fraction of the volume occupied by a given type of solvent molecule in the hydration shell and in the bulk solvent. The volume fraction of urea in the hydration shell is more than two times larger than in the bulk, whereas the volume fraction of TMAO in the hydration shell is only slightly larger in the binary solvent (TMAO + water) and becomes even less than in the bulk in the ternary solvent (TMAO + water + urea). Thus, TMAO tends to be excluded from the hydration shell of the protein. The behavior of the two cosolvents in the vicinity of the protein does not change much with pressure (from 1 to 5000 bar) and temperature (from 280 to 330 K). This is also in line with the conception of the "osmophobic effect" of TMAO to protect proteins from denaturation also at harsh environmental conditions. We also calculated the volumetric parameters of SNase and found that the cosolvents have a small but significant effect on the apparent volume and its contributions, *i.e.* the intrinsic, molecular and thermal volumes.

Received 18th November 2016,
Accepted 13th January 2017

DOI: 10.1039/c6cp07903b

www.rsc.org/pccp

Introduction

It is well known that the abundant osmolytes trimethylamine-*N*-oxide (TMAO) and urea influence the conformational equilibrium of proteins during folding/unfolding events. Addition of urea promotes denaturation of the protein biomolecules, while TMAO stabilizes the folded state by compensating a negative influence both of urea, and of environmental stresses such as high temperature and high pressure.[1–8] This phenomenon has been studied extensively by various experimental techniques, and recently also by computer simulations, to investigate the influence of the osmolytes (cosolvent molecules) on the properties of the protein on a molecular level.[9–12]

A general thermodynamic explanation of how a protector-osmolyte such as TMAO compensates environmental stress, was published by Bolen and co-authors.[3,13–15] Based on Gibbs energy measurements, it was proposed that the ability of osmolytes to stabilize proteins originates from an unfavorable interaction of the osmolyte with the protein, and this unfavorable interaction between a solvent component and the protein has been called the osmophobic effect.[14] If TMAO is "phobic" to the protein, then it clearly shows that the free energy of the solution in the presence of TMAO will be lower in the folded

[a] *Department of Cell and Molecular Physiology, Loyola University Chicago, Maywood, Illinois 60153, USA*
[b] *Institute of Chemical Kinetics and Combustion, SB RAS, 630090 Novosibirsk, Russia. E-mail: nikmed@kinetics.nsc.ru*
[c] *Novosibirsk State University, 630090 Novosibirsk, Russia*
[d] *Physikalische Chemie, Fakultät für Chemie und Chemische Biologie, Technische Universität Dortmund, Otto-Hahn-Strasse 4a, 44221 Dortmund, Germany. E-mail: roland.winter@tu-dortmund.de*

protein state, *i.e.* when it has less surface to interact with the ''osmophobic'' cosolvents.

In order to understand the osmolytes' influence at the molecular level, it is necessary to combine experimental data with results of molecular dynamics simulations (see, *e.g.*, the review by Canchi and Garcia[12]). Today, the nature of the protein–urea interaction is rather well understood. Urea is soluble in water in large concentrations and incorporates itself well in the hydrogen-bond network of water. It can accept and donate hydrogen bonds.[16–22] Urea accumulates in the vicinity of proteins owing to favorable direct interactions with them.[23,24] The direct interaction is a result of the favorable interaction of urea with all protein moieties, including the peptide backbone and side-chain groups by hydrogen bonds and also dispersion interaction.[25–35] Obviously, an unfolded protein has more possibilities for direct interactions with urea compared to a folded one, where large parts of the protein chain are buried inside the native structure. This provides an enthalpic driving force for unfolding, which shifts the equilibrium toward unfolded states of the protein in the presence of urea, as discussed for example in ref. 12 and 23.

The mechanism, how TMAO interacts with a protein seems to be more subtle. Indeed, both molecular dynamics simulations[26,36–38] and experiments[14,39–42] show that there is no favorable interaction between protein and TMAO. Moreover, TMAO exhibits a lower fraction in the protein hydration shell. This is less clear on a molecular level. Molecular dynamics simulations of CI2 (chymotrypsin inhibitor 2) in aqueous solution in the presence of urea and TMAO at high concentrations (8 M urea, 4 M TMAO and 4 M TMAO + 8 M urea) were reported.[36] Protein unfolding was obtained when urea directly interacted with the protein. However, some change of the hydration water structure was also marked. In the presence of TMAO, the native structure of the protein survived. In a recent work, molecular dynamics simulations of GB1 (a 16-residue β-hairpin) in different cosolvent mixtures (urea and TMAO) were performed.[26] In general, that work supports the findings by Bennion and Daggett.[36] It was pointed out that electrostatics plays a major role in denaturation by urea, suggesting that a direct interaction mechanism is operative. (Recall, the hydrogen bonds in classical molecular dynamics simulation are defined just as electrostatic interactions.) Urea causes denaturation of the initial conformation of the protein through the breaking of intra-protein hydrogen bonds, joining its terminal residues, whereas the TMAO interaction models of Kast *et al.*[43] and Canchi *et al.*[37] are offsetting the denaturing effect of urea. Obviously, the osmolytic nature of TMAO is defined by its specific interaction with water. The non-trivial nature of this interaction is determined by several contributions. First: the large dipole moment of the TMAO molecule, which strongly influences the water structure. The important role of the TMAO dipole moment was discussed by Schneck *et al.*[10] Second: the TMAO oxygen has the ability to make at ambient pressure up to three strong hydrogen bonds with water molecules. These hydrogen bonds have very distinct orientations and influence the structure of the water around TMAO's oxygen. Besides, experiments and *ab initio* molecular dynamics calculations showed that the mobility of those water molecules is significantly reduced compared to bulk water.[44–46] Third: TMAO molecules contain a significant hydrophobic part: three methyl groups. It is important to take into account all these different types of interactions of TMAO with water and the other molecules in solution. They act simultaneously, however in most studies, an emphasis is put only on one of them, such as hydrophobic interactions of TMAO with surfaces and hydrophobic molecules.[47–51]

The aim of this work is to establish general features of the distribution of urea and TMAO in the hydration shell of a protein and to investigate their influence on each other. We study the distribution of the molecules in the vicinity of the monomeric protein staphylococcal nuclease (SNase) in aqueous solution depending on the composition of the cosolvents and external conditions, temperature and pressure. For this, we performed all-atom molecular dynamics simulations of solutions, where SNase is in the native state for all the above conditions.

Methods

MD simulations outline

We performed all-atom molecular dynamics simulations of a SNase molecule in aqueous solution for a range of temperatures, pressures and cosolvent concentrations. The simulations were carried out using the GROMACS software package.[52,53] We used the OPLS force field[54] for the protein and the SPC/E water model.[55] For urea, we used a Kirkwood–Buff integral derived force field[56] and for TMAO we used the force field of Larini and Shea,[57] which is a modification of the potential of Kast *et al.*[43] It should be mentioned that recently another variant of this TMAO force field was derived for the use at higher pressures,[58] but this was not yet available, when we started the involved studies presented here. As described in our previous paper,[59] for the SNase residues we choose the protonation states corresponding to pH 7.0. The total charge of +8*e* on the protein was then neutralized by a uniform distribution of the opposite charge between all atoms in order to make the system neutral.

In view of the variety of force fields available in the literature, in a recent paper by F. Rodriguez-Ropero *et al.*,[60] different TMAO force fields and their impact on the folding of hydrophobic polymers at low TMAO concentrations were studied, and in summary it was concluded that the results obtained were qualitatively independent of the TMAO force field.

An initial energy minimization of the SNase structure was performed, starting from the crystallographic heavy atom coordinates[61] and using the steepest descent method for 1000 steps.[62] After that, the protein was solvated in a cubic box with a minimum distance of 15 Å from the surface of the protein to the closest face of the simulation box. For the system with cosolvents, we added an appropriate number of TMAO and/or urea molecules to reach the specific concentration. The Particle Mesh Ewald (PME) method[63,64] was used to calculate the electrostatic interactions, and a cut-off of 9 Å was used for the short-range van der Waals interactions. The MD simulations were carried out with an integration time step of 2 fs. After 1 ns equilibration, production runs were performed in the *NPT* ensemble[65,66] with relaxation

Table 1 Compilation of the aqueous SNase solutions studied. The upper line shows the cosolvent concentrations, the left columns show the pressures and the temperatures analyzed

	Pure water (K)	0.5 M TMAO (K)	1 M urea (K)	0.5 M TMAO + 1 M urea (K)	1 M TMAO (K)	2 M urea (K)	1 M TMAO + 2 M urea (K)
1 bar	280	300	300	300	280	280	280
	300				300	300	300
	330				330	330	330
2000 bar	300	300	300	300	300	300	300
5000 bar	300	300	300	300	300	300	300

times of 1.0 ps and 2.5 ps, respectively. The production run was carried out for 100 ns for each system. Snapshots for the analysis were saved each 1 ps.

Models of SNase in pure water were generated for T = 300 K at pressures p of 1, 2000, and 5000 bar, and for p = 1 bar at T = 280, 300, and 330 K. Models of aqueous solutions of SNase with cosolvents were simulated for 300 K at 1, 2000, and 5000 bar and the following cosolvent concentrations: 0.5 M TMAO, 1 M urea, 0.5 M TMAO + 1 M urea, 1 M TMAO, 2 M urea, 1 M TMAO + 2 M urea. Models for different temperatures were obtained for 1 bar at 280, 300 and 330 K for the compositions: 1 M TMAO, 2 M urea, and 1 M TMAO + 2 M urea. Thus, we generated and analyzed 29 solution models (see Table 1). The results, discussed in Section 3, mainly refer to systems with 1 M TMAO and 2 M urea as cosolvents.

It is known, that in real systems the SNase protein remains folded at all conditions that are covered by our simulations,[67,68] and this we also observe in our simulations. The radius of gyration of the SNase molecule indicates permanent fluctuations and we see slightly different mean values in the different simulation runs, but they all lie within the standard deviations of the other runs. Fig. 1 shows snapshots from our simulations of SNase in the presence of these cosolvents. In accord with the quantitative results which are presented later, one can see that the hydration shell of SNase is more populated by urea than by TMAO at the same cosolvent concentration (1 M).

Voronoi volume weighted distance distribution function

Other than atomic distance distribution functions, as they are usually calculated for solvent molecules around a protein, we used Voronoi volume-weighted distance distribution functions. To this end, we first construct the Voronoi tessellation of the solution (as we did it in our previous volumetric analysis of molecular dynamics models of various biomolecular solutions[59,69–75]). Then we assign to each heavy atom the volume of its cell on the Voronoi tesselation. Thus, every atom of a cosolvent gets a "weight" which is equal to its Voronoi volume. (For simplicity, the Voronoi volume of the covalently-bonded hydrogens is assigned to its heavy atom, see Fig. 2, center.) The weighted distance distribution function is calculated as a usual distance (or radial) distribution function, but each distance is weighted by the Voronoi volume of the current atom. (Recall, usually each atom is taken with a unit weight.)

The distances from the heavy atoms of the cosolvent molecule to the protein are measured from the center of the cosolvent atom to the surface of the closest protein atom, see Fig. 2, right. The surface of the protein atom is defined by its van der Waals sphere (a half of the Lennard-Jones parameter σ of the protein atom as its radius).

In this paper, we use the power (radical) Voronoi tessellation. It takes into account the size (radius) of the atoms, in contrast to the classical Voronoi tessellation. The volume of the power Voronoi regions can be calculated analytically with high efficiency (for details see ref. 69, 70 and 72). Note, the additively weighted Voronoi tessellation (S-tessellation) defines the volume assigned to a given atom mathematically more correctly than the power one. However, the volume of the S-regions can be calculated only numerically. Fortunately, the difference between the power- and S-tessellation is negligible if the radii of the atoms of the system do not differ greatly in magnitude. Real molecular systems satisfy this condition.

Volumetric characteristics

The apparent volume, V_{app}, the intrinsic volume, V_{int}, and the molecular volume, V_M, of the SNase molecule in solution were determined as described in our previous papers.[59,73,74] We obtained the apparent volume V_{app} of the solute, its partial molar volume at infinite dilution, by a variant of the Kirkwood–Buff integral method, based on the Voronoi tessellation of the surroundings of the solute molecule.[68,74,75] The intrinsic volume, V_{int}, was identified as the union of the Voronoi cells of all solute atoms (therefore V_{int} is also called the Voronoi

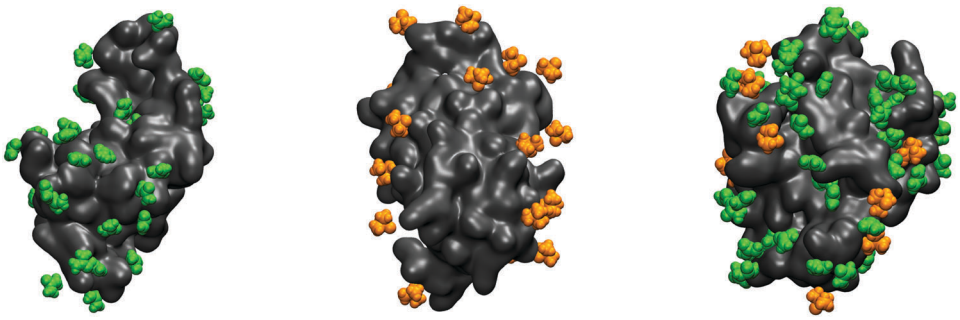

Fig. 1 Snapshots of SNase in aqueous solution with cosolvents in its hydration shell (d_{hyd} = 0.4 nm). Left: 1 M urea (green); in the center: 1 M TMAO (orange); right: 1 M TMAO + 2 M urea (T = 300 K, p = 1 bar).

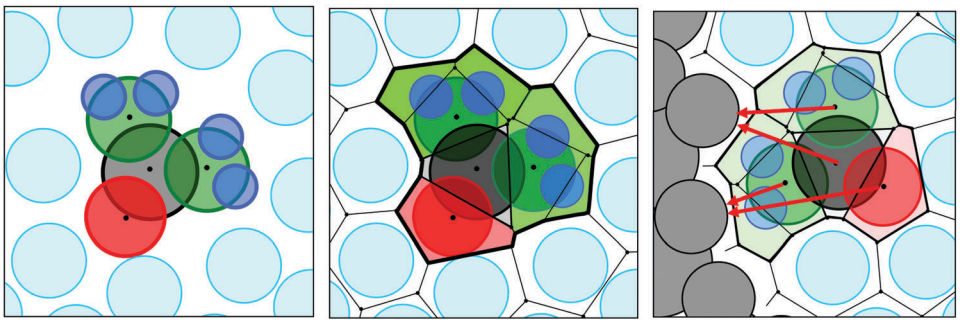

Fig. 2 2D illustration of a cosolvent molecule in solution. Left: A cosolvent molecule (cluster of color disks) among the water molecules (light-blue disks). Covalently-bonded hydrogens of the molecule are shown by dark-blue. Center: The Voronoi cells of this molecule. Voronoi cells of the covalently-bonded hydrogens are assigned to its heavy atoms (green). Right: Gray disks show surface atoms of a protein. The red arrows show distances from the heavy atoms of the cosolvent molecule to the closest atoms of the protein. This distance is measured from the center of the cosolvent atom to the surface of the closest protein atom.

volume, V_{Vor}, of the solute). The molecular volume, V_M (or van der Waals-volume of the solute), is the sum volume of all its fused atomic spheres plus the volume of internal cavities.[59,73] From these properties we can get two derived quantities: $\Delta V = V_{app} - V_{int}$, the contribution of the solvent to V_{app},[76,77] *i.e.*, the volume change due to the density change in the surrounding solvent under the influence of the solute,[59,73] and $V_{TI} = V_{app} - V_M$, the contribution of the total environment of the solute to its apparent volume, which may also be associated with the thermal volume, V_T, as introduced by Chalikian[78] (for details see ref. 75).

Orientation to the protein

To study the orientation of a cosolvent molecule with respect to the protein, we calculated an occurrence probability function for the cosine of the angle α between the dipole vector of the cosolvent molecule and the direction from the center atom of the molecule to the protein.

The dipole direction vector is drawn from the central atom of the molecule (C for urea and N for TMAO) to the oxygen atom of the molecule, Fig. 3. The direction to the protein is defined by the vector pointing from the central atom of the cosolvent molecule to the nearest atom of the protein.

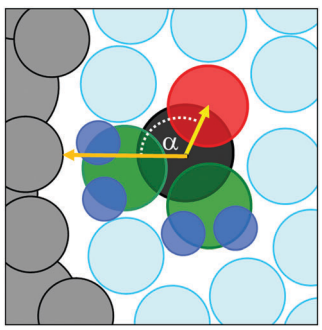

Fig. 3 Orientation of a cosolvent molecule (TMAO or urea) at the protein molecule. The angle α is measured between the vector pointing from the central atom of the molecule to the oxygen atom (dipole moment direction), and the vector directed from the center to the surface of the closest protein atom.

Results

Volumetric analysis

The apparent (V_{app}), intrinsic (V_{int}) and molecular (V_M) volumes of SNase in our solutions are shown in Fig. 4a and b as functions of pressure and temperature. First of all, we remark that these volumetric parameters and the coefficients of thermal expansion and isothermal compressibility in pure water (blue curves) are very close to the values obtained in our previous papers, where we used smaller systems of aqueous solutions of SNase.[59,75] Second, one can see a small, but systematic influence of the cosolvents on the volumetric parameters.

The observed shifts can be explained in the following way: (i) intrinsic volume: the addition of cosolvents decreases V_{int} and this decrease is stronger for urea (green lines) than for TMAO (red lines). This can be explained by the fact that urea approaches SNase more closely than TMAO (as will be shown later). By this, the free volume around SNase (the additional empty space assigned to the protein, as a part of the Voronoi volume, recall $V_{int} = V_{Vor}$) is more restricted by urea. In the ternary solvent, the decrease of V_{int} is further enlarged. (ii) Apparent volume: in contrast to V_{int}, V_{app} increases by the presence of TMAO for all temperatures. This is because ΔV increases with TMAO (see particularly Fig. 5). It can be explained by the fact that TMAO contains hydrophobic groups and that the water in hydrophobic hydration shells resembles lower density, 'locally stretched', water.[79] In consequence, a positive cosolvent contribution to $\Delta V = V_{app} - V_{int}$ (see red and black lines in Fig. 5) is a signature of the hydrophobically hydrated part of amphiphilic molecules.[74] By contrast, urea, which is easily incorporated into the hydrogen-bond network of water (see also below), produces an opposite effect on V_{app} (compare the red and green lines in Fig. 4b). Finally, the black line in Fig. 4b shows the counteraction of the two effects: a mutual cancellation of the influence of urea and TMAO on V_{app}. Interestingly, these opposite shifts are in accordance with the well-known opposing effect of urea and TMAO on protein denaturation. A similar behavior as in Fig. 4 is observed also for 0.5 M TMAO, 1 M urea, and their mixture (not shown here). (iii) Molecular volume: V_M changes less and unregularly. This volume term does not

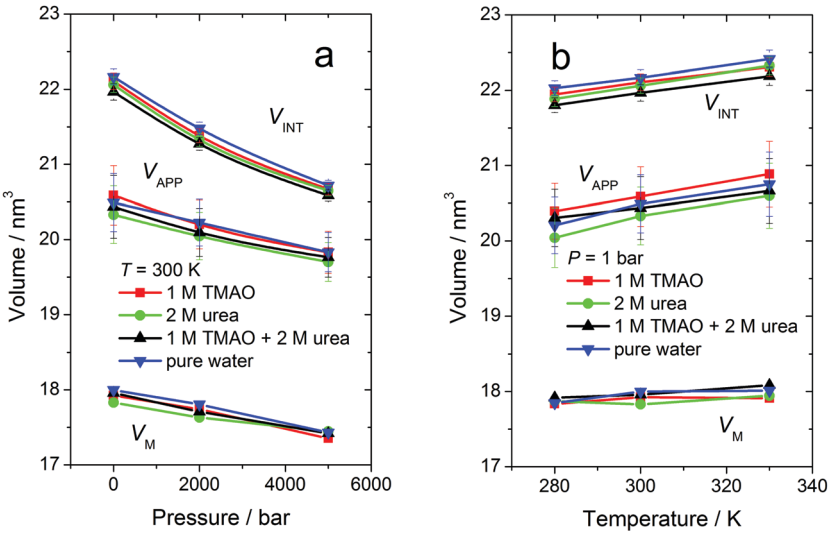

Fig. 4 The apparent (V_{app}), intrinsic ($V_{int} = V_{Vor}$) and molecular (V_M) volumes of the SNase molecule in different solutions as a function of pressure (a) and temperature (b). The colors of the curves specify the solvents: pure water (blue), water with 1 M TMAO (red), water with 2 M urea (green), water with 1 M TMAO and 2 M urea (black).

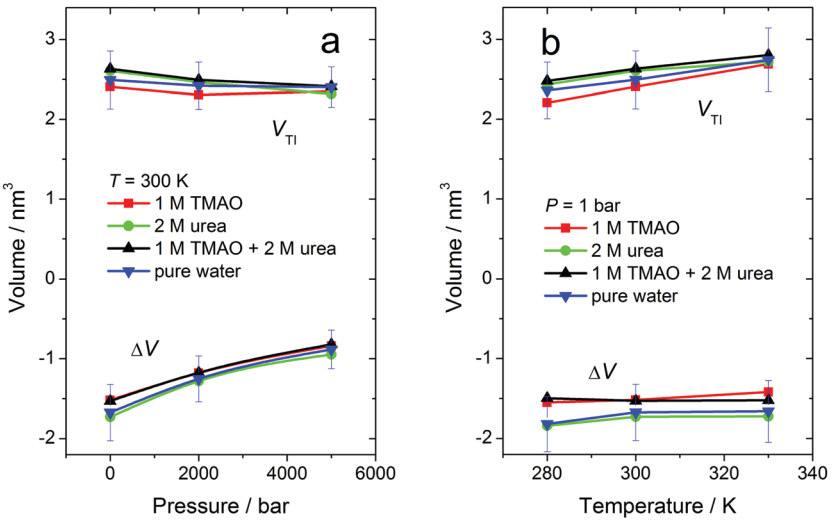

Fig. 5 The thermal volume ($V_{TI} = V_{app} - V_M$), and the contribution of the solvent to the apparent volume ($\Delta V = V_{app} - V_{int}$) of the SNase molecule in different solutions as functions of pressure (a) and temperature (b). See captions in Fig. 4.

contain surface free space. Small changes in V_M can hence be a result of small conformational variations of the protein, where, for example, some pockets turn to internal voids and *vice versa*.

Using the data of Fig. 4, we can calculate the "thermal" volume, V_{TI}, of the protein and the contribution of the solvent ΔV as it was introduced in Section 2.3. Fig. 5 depicts these values for our models also as function of pressure and temperature.

As in our previous papers,[59,75] we see a linear increase of the thermal volume V_{TI} of SNase with temperature, and a small decrease with pressure (Fig. 5a and b). As discussed there, this is due to an expansion of the free space at the solute–solvent interface with temperature and only a slight compression with pressure. The addition of urea (green and black lines) increases the thermal volume, and the addition of TMAO (without urea) decreases it (red lines). To explain it, let us write the thermal volume as $V_{TI} = V_B^M + \Delta V$ (formula (17) in ref. 75), where $V_B^M = V_{int} - V_M$ has been introduced as the boundary empty volume assigned to the protein. Obviously, this value is greater for elongated and less for compact conformations of a protein molecule. If ΔV coincides for different solutions (see the couples of red and black, and also of blue and green lines in Fig. 5) then the change of V_{TI} is solely due to V_B^M. Thus, one may conclude that the conformations of SNase in solution with urea are slightly "extended" in comparison with pure water and water with TMAO. However, this is a very small effect. As mentioned in Section 2.1, the SNase molecule is natively folded in our simulations. Of course, small fluctuations of the gyration radius of SNase emerge, but the mean values are very close for all solutions.

As we have seen in Fig. 5, ΔV, which reflects the contribution of the hydration water only, demonstrates again a clear difference between urea and TMAO. The coincidence of the blue and green lines reveals that the addition of urea does not change ΔV compared to pure water as solvent. This is in agreement with different experiments showing that urea is incorporated into the water structure without much disturbance, behaving "water like", it "fits well into the water network" (see ref. 80–84, and others). In contrast, the addition of TMAO to the pure aqueous solvent (compare blue and red lines) increases ΔV. The influence of TMAO is nearly the same also in the ternary solvent (black lines). As discussed above, this reflects the influence of the hydrophobic hydration shell of TMAO on the hydration water of SNase. Please note, the increase of ΔV with the addition of TMAO can also counteract the overall effect of pressure on the apparent volume of the protein. This observation may help to understand the stabilizing influence of TMAO with respect to pressure denaturation.

The influence of the cosolvents on the volumetric parameters, as discussed here, is rather small, however our considerations are in line with the current interpretation of the experimentally observed properties of TMAO and urea in the vicinity of a protein.

Cosolvent volume distributions

The Voronoi volume-weighted distance distributions of the heavy atoms of the cosolvents and water around SNase for different pressures at $T = 300$ K are shown in Fig. 6. Roughly speaking, they represent the volume occupied by the different cosolvent species in the environment of the protein. The integral of these curves over an interval of distance r yields the volume occupied by the considered cosolvent species in this interval. Thus, in short, we will call them the "volume distributions".

For both cosolvents, the location of the first peak is shifted slightly to smaller distances at high pressures, whereas the first peak position of water does not move with increasing pressure, as known from the oxygen–oxygen pair distribution function of pure water.[85] This behavior is similar for higher (Fig. 6a) and lower (Fig. 6d) cosolvent concentrations. Only the height of the peaks changes with the changing concentrations.

Urea exhibits a unimodal broad peak with a maximum at 0.177 nm, which extends over a region from about 0.1 to 0.4 nm. On the contrary, TMAO has a doublet, a first sharp sub-peak at 0.194 nm, and a second one is located at around 0.37 nm. The second peak is mainly produced by the TMAO oxygen, whereas the first one is produced by the methyl groups, as one can see in Fig. 12 in the next section, where the conventional non-weighted distributions of the heavy atoms and the orientations of the cosolvent molecule are discussed. Water also has a unimodal first peak, appearing at 0.137 nm from the protein surface.

When urea is added to the TMAO solution, the TMAO peaks are slightly smeared out and their height decreases, especially the first peak at high pressures (Fig. 6b and c). On the contrary, the urea distribution is less affected in the ternary system (Fig. 6a and c). In summary, the volume distributions of water and the 'water like' urea are not much changed by the addition

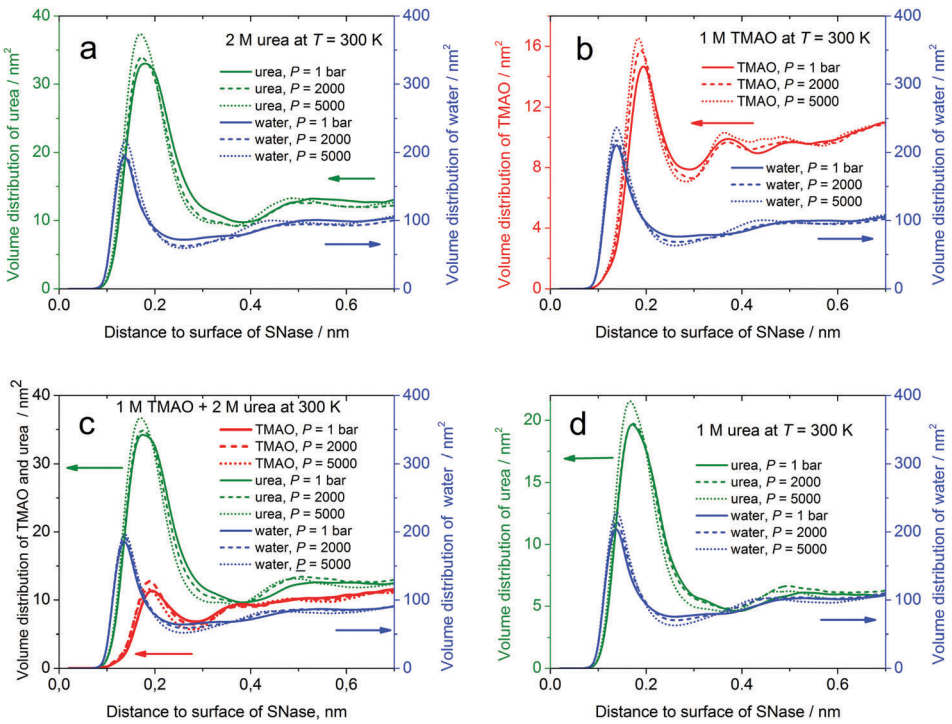

Fig. 6 Volume distribution of the cosolvent and water molecules around SNase at 300 K for different pressures. 2 M urea in water (a), 1 M TMAO in water (b), 1 M TMAO + 2 M urea in water (c), 1 M urea in water, (d) blue curves for water, green for urea, red for TMAO. Pressure: 1 bar (solid lines), 2000 bar (dashed), 5000 bar (dotted). The scale for water is shown on the right.

of TMAO, whereas the volume distribution of TMAO is more sensitive to the addition of urea. These changes are reflected in the average number of cosolvent molecules within the 0.4 nm shell around the protein and will be discussed in more detail in conjunction with Fig. 8.

The temperature dependence of the volume distribution functions at 1 bar is shown in Fig. 7. In contrast to the pressure dependence, the peak positions of all components are rather temperature independent in the given temperature interval covered. The height of the urea peak changes as expected: increased thermal motions broaden the peak slightly and thus decrease the peak height with temperature. Remarkably, the temperature dependence of the TMAO peak is opposite (Fig. 7b): the peak heights increase with temperature. This is a clear indication for the hydrophobic interaction between TMAO and the SNase surface and well known from simpler aqueous solutions (see ref. 86 and 87, and references given there).

Fig. 8 complements these observations by giving the average number of urea and TMAO molecules in the solvation shell of SNase for different pressures and temperatures. Molecules with centers closer than 0.4 nm to the protein surface were counted (the nitrogen atom was considered as center of TMAO and the carbon atom as a center of urea). One can clearly see that the number of the cosolvent molecules in the solvation shell of SNase increases with pressure in all our solutions (Fig. 8a), whereas with temperature, the number of urea molecules decreases, but the number of TMAO increases (Fig. 8b). This increasing number of TMAO molecules in the vicinity of SNase with temperature (red lines of Fig. 8b) indicates again a predominantly hydrophobic interaction between TMAO and the protein. The decreasing number of urea with temperature is usually interpreted as indication of a predominantly enthalpic interaction. Fig. 8 also reveals a strong accumulation of urea in the protein hydration shell, compared to TMAO: the number of urea molecules (about 64, green lines) roughly quadruplicates the number of TMAO (about 16, red lines), although its overall concentration is only double the TMAO concentration.

Upon the addition of a second cosolvent, some systematic behavior can be observed in Fig. 8, which is in accord with the behavior of the volume distribution functions presented in Fig. 6 and 7. First, at low cosolvent concentrations (blue and magenta lines in Fig. 8a) the addition of a second cosolvent does not influence the concentration of the first one. Second, even at higher concentrations, the urea concentration is not much influenced by the addition of TMAO (green lines). Third, in contrast, a marked influence is seen on TMAO at higher concentrations (dotted and solid red lines in Fig. 8a and b). Thus, urea strongly affects the TMAO distribution at the SNase surface, whereas the TMAO influence on the volume distribution of urea at the protein interface is much smaller. This observation is in line with recent simulation studies on the influence of urea on the hydrophobic interaction.[23] When comparing with other simulation studies,[88] one should keep in mind, that the accumulation/depletion effect observed here is effective at higher concentrations, only.

Fig. 9 shows the volume fractions, $f_i(r)$, occupied by urea or TMAO around SNase in the binary and ternary solvent mixtures. As discussed above, our Voronoi volume-weighted

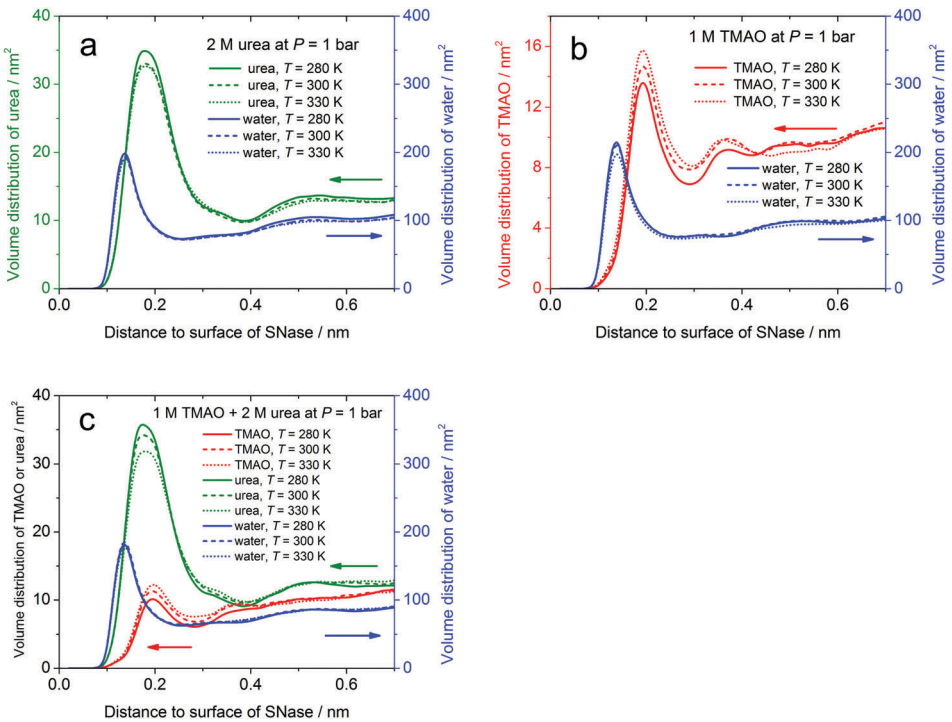

Fig. 7 Volume distribution of the cosolvents and water molecules around SNase for different temperatures at p = 1 bar. Solid lines for T = 280 K, dashed lines for T = 300 K, dotted lines for T = 330 K.

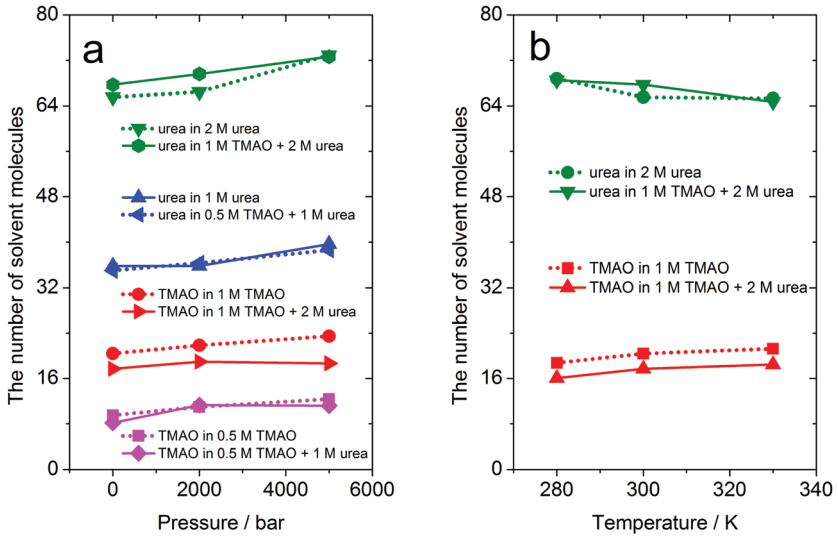

Fig. 8 Number of cosolvent molecules in the hydration shell of SNase ($r < 0.4$ nm) as a function of pressure at 300 K (a) and as a function of temperature at 1 bar (b). Solid lines: ternary solvents, dotted lines: binary solvents. Green and blue for urea, red and magenta for TMAO.

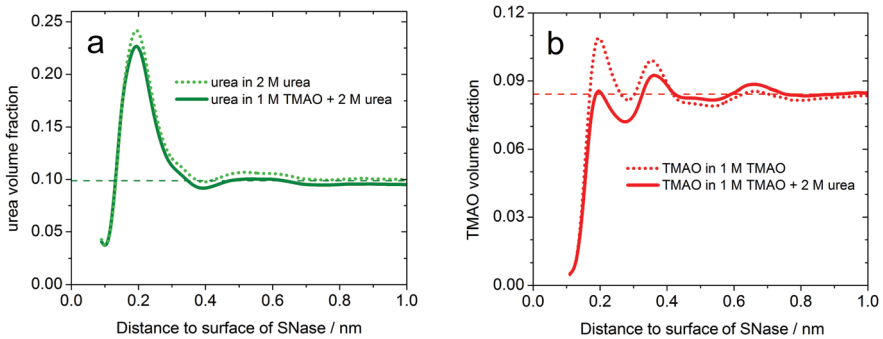

Fig. 9 Volume fraction, $f_i(r)$, occupied by the cosolvent molecules around SNase, (a) urea, (b) TMAO. Dotted lines: binary solvents (2 M urea in water, and 1 M TMAO in water). Solid lines: ternary solvent (1 M TMAO + 2 M urea in water). T = 300 K, p = 1 bar.

distance distribution functions, $v_i(r)$, represent the volume occupied by the cosolvent molecules of species i, which are found in a layer with thickness Δr at distance r. As we use Voronoi volumes, we divide up the whole space between the cosolvents without any overlapping and gaps. Accordingly, we can define a volume fraction, $f_i(r)$ of a cosolvent in any part of solution, according to $f_i(r) = v_i(r)/(v_{TMAO}(r) + v_{urea}(r) + v_{water}(r))$.

Beyond a distance of 0.8 nm, both urea and TMAO reach asymptotically the bulk value of their volume fractions. At shorter distances, the volume fraction of urea is nearly unchanged for the binary and ternary solvent mixtures (Fig. 9a). This shows again that the position of urea is rather insensitive to the presence of TMAO at these concentrations. On the other hand, the volume fraction of TMAO differs for the binary and ternary solvents, Fig. 9b. Interestingly, the fraction of TMAO in the hydration shell of SNase is always much lower than that of urea, and for the ternary solvent it is even less than in the bulk (see the solid red line in Fig. 9b). This depletion of TMAO has also been observed before by other groups.[88] On the other hand, the volume fraction of urea in the hydration shell is substantially larger than in the bulk, and this is true for both the binary and ternary solvent mixture (Fig. 9a).

Next we discuss the temperature dependent data. Fig. 10a shows the volume fractions in the binary solvents for different temperatures, and Fig. 10b the corresponding data for the ternary ones. The most prominent feature is the opposite behavior of urea and TMAO with increasing temperature: the volume fraction for urea decreases, and that for TMAO increases. This clearly indicates again an enthalpic interaction of urea with the protein and an essentially entropy driven hydrophobic interaction of TMAO with the protein interface.

Cosolvent orientation

In this section we discuss the dipole orientation distribution functions of the cosolvent molecules in the solvation shell of SNase. Additionally, we use conventional (non-weighted) distance distributions of the heavy cosolvent atoms around the protein to yield information on the molecular orientations. The distance to the protein is also measured to its surface, as described in Section 2.2. As we see, there is some difference

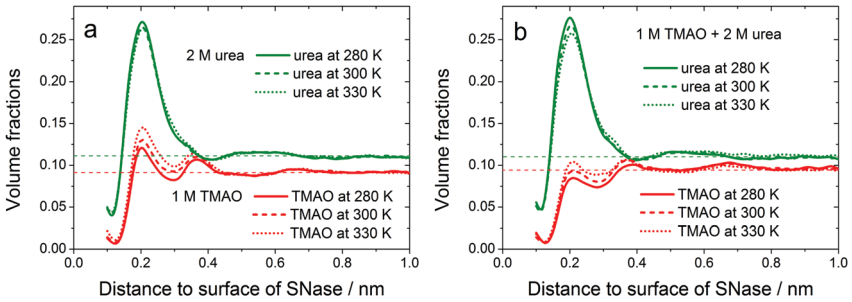

Fig. 10 Volume fraction occupied by urea and TMAO at different temperatures solid lines for T = 280 K, dashed lines for T = 300 K, dotted lines for T = 330 K.

between the volume-weighted and the non-weighted distributions. This is because the Voronoi volumes of the cosolvent atoms differ from each other, especially for TMAO (compare the dotted curve in Fig. 12a and the solid red curves in Fig. 6b).

Fig. 11a shows the distance distributions for the heavy atoms of urea at 1 bar and 300 K. We can discuss them together with the orientation distributions in Fig. 11b, where the occurrence probability for the cosine of the angle α between the dipole vector of urea and the vector pointing from the C atom to the nearest atom of SNase are shown (see Section 2.4). We divided the hydration shell of SNase into three sub-shells, comprising molecules with a distance of their central carbon atom to the protein surface from 0 to 0.2 nm, from 0.2 to 0.3 nm, and from 0.3 to 0.4 nm. One can clearly identify two kinds of preferential orientations in the first two sub-shells: (i) a narrow peak at $\cos\alpha \approx -1$, showing that some urea molecules orient their dipoles away from the SNase; (ii) a broad peak from $\cos\alpha \approx -0.5$ to $\cos\alpha \approx +0.5$. This means that the majority of urea is oriented roughly parallel to the SNase, with variances of α from −60 to +60 degrees. In the third sub-shell we observe a uniform distribution of orientations (Fig. 11b, blue curve).

Thus, in combination with the N, O, and C peak positions shown in Fig. 11a, we can say that an orientational bias can only be observed for the nearest urea molecules that are closer than 0.3 nm to the SNase surface. Some of them are in contact with the protein simultaneously by both amino groups, with the oxygen directed outside (these oxygens correspond to the small shoulder of the red curve in Fig. 11a at 0.35 nm). However most of the molecules are in contact with the protein both by the oxygen and one of the amino groups (they correspond to the main peaks of the black and red curves at around 0.15 in Fig. 11a).

TMAO displays a quite different behavior (see Fig. 12). The main maximum of the oxygen distance distribution in Fig. 12a is located between 0.3 and 0.4 nm (red curve). In combination with the positions of the main peaks of the methyl carbon and the nitrogen distributions (blue and black lines), which appear at shorter distances, we assume that a majority of the TMAO molecules is pointing away from the protein with its oxygen, at least some of their methyl groups being in close contact with the protein. This interpretation is supported by the angular distributions in Fig. 12b. For the molecules with a nitrogen distance between 0.2 and 0.3 nm (the main nitrogen peak in the distance distribution) we observe a pronounced peak at $\cos\alpha \approx -1$, accompanied by a broad distribution of negative cosine-values (green line). All these molecules tend to point away from the protein surface with their oxygen, many of them almost exactly radially outwards. In this case, all three methyl groups have to be in contact with the protein surface. However, there is also an appreciable fraction of TMAO molecules with an oxygen which is closer to the protein surface than the central N atom: there appears a small pronounced peak at 0.13 nm on the oxygen distance distribution, Fig. 12a. The broad maximum in Fig. 12b at $\cos\alpha \approx 0.7$ (angles between 30 and 65 degrees) indicates a preferential orientation of molecules, which can be

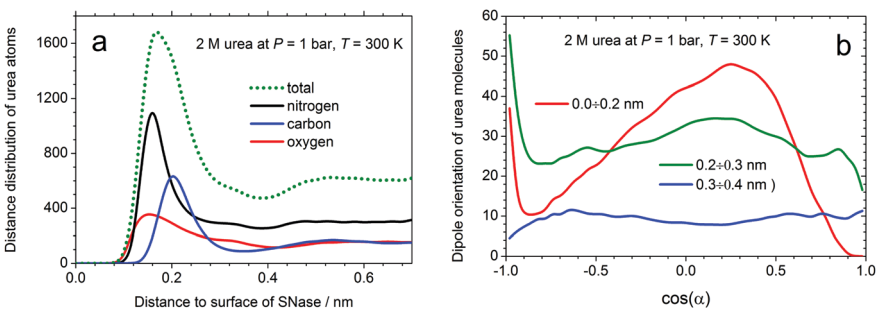

Fig. 11 (a) Partial and total distance distributions for heavy atoms of urea around SNase. Nitrogen: black, carbon: blue, oxygen: red. Dotted line shows the total (sum) distribution. (b) Dipole orientation distribution in consecutive subshells around SNase, see text (distances are measured from the central carbon atom to the protein surface).

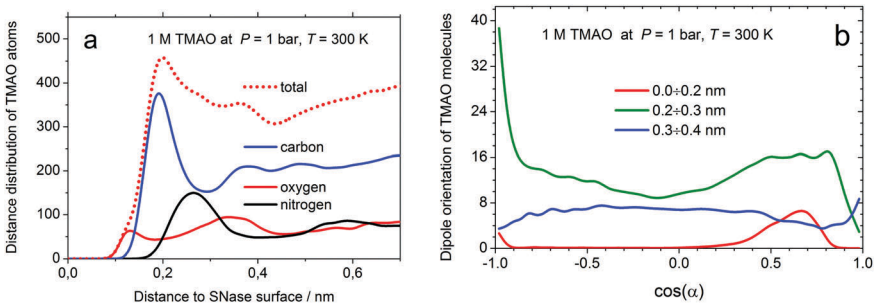

Fig. 12 (a) Partial and total distance distributions for the heavy atoms of TMAO around SNase (nitrogen atoms (black), carbon (blue), oxygen (red)). The dotted line is the total (sum) distribution. (b) Dipole orientation distribution in subsequent subshells around SNase (distances from the central N atom to the protein surface).

described as ''lying sideways'', *i.e.* in contact with the protein surface by one or two methyl groups, as well as with the oxygen atom. The latter orientations are in line with the results of two recent studies on the orientation of TMAO at hydrophobic surfaces. A combined experimental and simulation study[89] revealed a preferential ''side-on'' (''sideway'') orientation, and the vibrational sum frequency spectroscopy (VSFS) study of Sagle *et al.*[90] are interpreted in terms of TMAO molecules with orientations between 0° and 90° to the surface normal. This would correspond to our orientations between 30° and 65°. Both orientations comprise methyl groups that are in contact to the surface and can thus give rise to hydrophobic interactions. Making such comparisons, we have to keep in mind, that in our system we do not have a homogeneously hydrophobic or free surface. The protein surface has many hydrophilic parts and also spots for hydrogen-bonding. The orientational distributions shown are averages over all cosolvent molecules in the vicinity of the protein. Correspondingly, we expect to have a broad distribution of orientations.

For more distant TMAO molecules, we see a less pronounced distribution of the orientations (blue curve in Fig. 12b), but with a clear inverse behavior, compared to the previous curves (red and green): we see minima where there were maxima, and a maximum at $\cos\alpha \approx 1$ where there is a minimum in the distributions of the closer molecules. These TMAO molecules with a nitrogen distance of more than 0.3 nm cannot be in contact with the protein. The observed orientational peculiarities can result from water mediation. For example, the peak at $\cos\alpha \approx 1$ (reverse orientation of the TMAO molecule with its oxygen pointing to the protein, and the methyl group outwards) can be produced by water molecules forming hydrogen bonds simultaneously with the protein and the TMAO oxygen. However, these details need additional analysis.

Conclusions

In this paper we studied the hydration shell of a well characterized monomeric protein, SNase, using molecular dynamics simulation models of aqueous solutions with TMAO and urea molecules as cosolvents. Volumetric characteristics of SNase, such as the apparent volume and its components, atomic distance distributions and Voronoi volume-weighted distance distributions of the cosolvent molecules in the surroundings of the protein and their orientations were calculated for different temperatures, pressures, and compositions of the solutions. The data obtained help us to reveal a general picture of the cosolvent arrangement around the protein including extreme environmental conditions. We observe a reverse, antagonistic behavior of these two cosolvent species in the hydration shell of the protein. Our calculations confirm and illustrate on the molecular level the ''classical'' thermodynamic interpretation of the role of these cosolvents in their propensity to denature or stabilize the folded state of SNase in terms of the osmophobic effect.[14] According to this point of view, the ability of a cosolvent to stabilize proteins originates from the unfavorable interaction of this molecule with the protein.

We used the Voronoi tesselation technique, developed in previous papers for the volumetric characterization of biomolecular solutions with pure water as solvent, to calculate the volumetric parameters of SNase in the presence of cosolvents, *i.e.*, the apparent, intrinsic, molecular and thermal volumes, and the contribution of the cosolvents to the apparent volume. Additionally, we introduced, on the basis of the Voronoi tessellation, the calculation of Voronoi volume-weighted distribution functions of the cosolvent molecules, which describe the distribution of the volumes occupied by the cosolvents in a quantitative way.

We found that the cosolvents have a small, but discernible influence on the volumetric parameters of the solute biomolecule. The small systematic changes with the composition of the solvent can be explained by the presence of these cosolvents in the close proximity of the protein. The Voronoi volume-weighted distribution functions indicate clearly a remarkable qualitatively different behavior of urea and TMAO in the vicinity of the protein. The distribution of urea in the hydration shell of SNase is very stable: the volume distribution of this 'water like' molecule varies very little with pressure and temperature, and it is not much changed by the addition of TMAO. In contrast, the volume distribution of TMAO is very sensitive to the addition of urea: by the addition of urea, TMAO is depleted in the vicinity of SNase. In consequence, whereas the volume fraction of urea in the hydration shell is always substantially larger than in the bulk, in the ternary solvent the volume fraction of TMAO in the hydration shell does not differ much from the bulk. More quantitatively: the volume fraction of urea is in the binary and in the ternary solvent more than a factor

of two larger in the hydration shell than in the bulk solvent, whereas in the binary solvent (TMAO + water) the fraction of TMAO in the hydration shell is only slightly larger and becomes even less than that in the bulk in the ternary solvent (TMAO + water + urea). This depletion is not observable at lower concentrations, as one can clearly deduce from the number of cosolvent molecules in the hydration shell of SNase.

The mechanism behind this peculiar behavior can be understood, when considering the temperature dependence of the volume distributions and the orientational distributions of the cosolutes in the vicinity of the protein. The opposite temperature dependence of the volume distributions of TMAO and urea indicate a dominating hydrophobic (entropy driven) interaction with TMAO and a prevailing enthalpic interaction of urea with SNase. This is confirmed by the preferential orientation of TMAO with its hydrophobic methyl groups in contact with the SNase surface. Obviously, the enthalpic interaction of urea (the oxygen atom and the amino groups of urea are very often simultaneously in contact with the protein) is dominating over the hydrophobic interaction of TMAO, thus leading to the observed expulsion of TMAO upon addition of urea. This is the so called ''osmophobic'' effect, underlying presumably the action of stabilizing osmolytes.

As discussed intensively in the literature, such a depletion of a cosolvent can lead to an effectively attractive depletion interaction of macromolecules,[91,92] either intra- or inter-chain, thus promoting (intramolecular) compaction or (intermolecular) aggregation. In the case of proteins this would support and stabilize folding. Surely, in our simulations the interaction of SNase and the TMAO molecules (the depletants) is predominantly hydrophobic, as we discussed, but from this we cannot conclude definitely, whether the resulting effective attractive intra- or inter-polymeric depletion forces are of enthalpic or entropic nature.[93,94] To answer this question, the calculation of temperature dependent potentials of mean force would be necessary, but this is outside the scope of our study.

Interestingly, the structural characteristics of the two cosolvents in the vicinity of the protein does not change much with pressure (from 1 to 5000 bar) and temperature (from 280 to 330 K). This is also in line with the conception of the ''osmophobic effect'' of TMAO to protect proteins from denaturation also at harsh environmental conditions, such as in the deep sea, where pressures up to the 1 kbar level are encountered.

Acknowledgements

Financial support from grants RFFI (No. 15-03-03329), the DFG research unit FOR 1979, and the Cluster of Excellence RESOLV (EXC 1069) funded by the Deutsche Forschungsgemeinschaft is gratefully acknowledged.

References

1 P. H. Yancey, M. E. Clark, S. C. Hand, R. D. Bowlus and G. N. Somero, *Science*, 1982, **217**, 1214–1222.
2 S. N. Timasheff, *Annu. Rev. Biophys. Biomol. Struct.*, 1993, **22**, 67–97.
3 A. Wang and D. W. Bolen, *Biochemistry*, 1997, **36**, 9101–9108.
4 L. A. Benton, A. E. Smith, G. B. Young and G. J. Pielak, *Biochemistry*, 2012, **51**, 9773–9775.
5 M. A. Schroer, Y. Zhai, D. C. F. Wieland, C. J. Sahle, J. Nase, M. Paulus, M. Tolan and R. Winter, *Angew. Chem., Int. Ed.*, 2011, **50**, 11413–11416.
6 P. H. Schummel, A. Haag, W. Kremer, H. R. Kalbitzer and R. Winter, *J. Phys. Chem. B*, 2016, **120**, 6575–6586.
7 C. Rosin, K. Estel, J. Hälker and R. Winter, *ChemPhysChem*, 2015, **16**, 1379–1385.
8 F. Meersman, D. Bowron, A. K. Soper and M. H. J. Koch, *Biophys. J.*, 2009, **97**, 2559–2566.
9 P. Ganguly, N. F. A. van der Vegt and J.-E. Shea, *J. Phys. Chem. Lett.*, 2016, **7**, 3052–3059.
10 E. Schneck, D. Horinek and R. R. Netz, *J. Phys. Chem. B*, 2013, **117**, 8310–8321.
11 B. Moeser and D. Horinek, *J. Phys. Chem. B*, 2014, **118**, 107–114.
12 D. R. Canchi and A. E. García, *Annu. Rev. Phys. Chem.*, 2013, **64**, 273–293.
13 Y. Liu and D. W. Bolen, *Biochemistry*, 1995, **34**, 12884–12891.
14 D. W. Bolen and I. V. Baskakov, *J. Mol. Biol.*, 2001, **310**, 955–963.
15 D. W. Bolen and G. Rose, *Annu. Rev. Biochem.*, 2008, **77**, 339–362.
16 K. A. Sharp, B. Madan, E. Manas and J. M. Vanderkooi, *J. Chem. Phys.*, 2001, **114**, 1791–1796.
17 Y. L. A. Rezus and H. J. Bakker, *Proc. Natl. Acad. Sci. U. S. A.*, 2006, **103**, 18417–18420.
18 S. Paul and G. N. Patey, *J. Am. Chem. Soc.*, 2007, **129**, 4476–4482.
19 M. C. Stumpe and H. Grubmueller, *J. Phys. Chem. B*, 2007, **111**, 6220–6228.
20 H. Kokubo and B. M. Pettitt, *J. Phys. Chem. B*, 2007, **111**, 5233–5242.
21 J. K. Carr, L. E. Buchanan, J. R. Schmidt, M. T. Zanni and J. L. Skinner, *J. Phys. Chem. B*, 2013, **117**, 13291–13300.
22 D. Bandyopadhyay, S. Mohan, S. K. Ghosh and N. Choudhury, *J. Phys. Chem. B*, 2014, **118**, 11757–11768.
23 R. Zangi, R. Zhou and B. J. Berne, *J. Am. Chem. Soc.*, 2009, **131**, 1535–1541.
24 H. Wei, Y. Fan and Y. Q. Gao, *J. Phys. Chem. B*, 2010, **114**, 557–568.
25 A. Caballero-Herrera, K. Nordstrand, K. D. Berndt and L. Nilsson, *Biophys. J.*, 2005, **89**, 842–857.
26 G. Borgohain and S. Pau, *J. Phys. Chem. B*, 2016, **120**, 2352–2361.
27 B. J. Bennion and V. Daggett, *Proc. Natl. Acad. Sci. U. S. A.*, 2003, **100**, 5142–5147.
28 L. Hua, R. H. Zhou, D. Thirumalai and B. J. Berne, *Proc. Natl. Acad. Sci. U. S. A.*, 2008, **105**, 16928–16933.
29 D. Horinek and R. R. Netz, *J. Phys. Chem. A*, 2011, **115**, 6125–6136.

30 M. C. Stumpe and H. Grubmuller, *J. Am. Chem. Soc.*, 2007, **129**, 16126–16131.
31 S. Lee, Y. L. Shek and T. V. Chalikian, *Biopolymers*, 2010, **93**, 866–879.
32 E. J. Guinn, L. M. Pegram, M. W. Capp, M. N. Pollock and M. T. Record, *Proc. Natl. Acad. Sci. U. S. A.*, 2011, **108**, 16932–16937.
33 D. R. Canchi, D. Paschek and A. Garcıa, *J. Am. Chem. Soc.*, 2010, **132**, 2338–2344.
34 D. R. Canchi and A. E. Garcıa, *Biophys. J.*, 2011, **100**, 1526–1533.
35 L. Ma, L. Pegram, M. T. Record Jr. and Q. Cui, *Biochemistry*, 2010, **49**, 1954–1962.
36 B. J. Bennion and V. Daggett, *Proc. Natl. Acad. Sci. U. S. A.*, 2004, **101**, 6433–6438.
37 D. R. Canchi, P. Jayasimha, D. C. Rau, G. I. Makhatadze and A. E. Garcia, *J. Phys. Chem. B*, 2012, **116**, 12095–12104.
38 R. Sarma and S. Paul, *J. Phys. Chem. B*, 2013, **117**, 9056–9066.
39 T. Y. Lin and S. N. Timasheff, *Biochemistry*, 1994, **33**, 12695–12701.
40 E. S. Courtenay, M. W. Capp, C. F. Anderson and M. T. Record, *Biochemistry*, 2000, **39**, 4455–4471.
41 Q. Zou, B. J. Bennion, V. Daggett and K. P. Murphy, *J. Am. Chem. Soc.*, 2002, **124**, 1192–1202.
42 J. Hunger, K. J. Tielrooij, R. Buchner, M. Bonn and H. J. Bakker, *J. Phys. Chem. B*, 2012, **116**, 4783–4795.
43 K. M. Kast, J. Brickmann, S. M. Kast and R. S. Berry, *J. Phys. Chem. A*, 2003, **107**, 5342–5351.
44 S. Imoto, H. Forbert and D. Marx, *Phys. Chem. Chem. Phys.*, 2015, **17**, 24224–24237.
45 K. Usui, J. Hunger, M. Sulpizi, T. Ohto, M. Bonn and Y. Nagata, *J. Phys. Chem. B*, 2015, **119**, 10597–10606.
46 J. Hunger, N. Ottosson, K. Mazur, M. Bonn and H. J. Bakker, *Phys. Chem. Chem. Phys.*, 2015, **17**, 298–306.
47 C. Stanley and D. C. Rau, *Biochemistry*, 2008, **47**, 6711–6718.
48 L. B. Sagle, K. Cimatu, V. A. Litosh, Y. Liu, S. C. Flores, X. Chen, B. Yu and P. S. Cremer, *J. Am. Chem. Soc.*, 2011, **133**, 18707–18712.
49 S. Paul and G. N. Patey, *J. Phys. Chem. B*, 2007, **111**, 7932–7933.
50 S. Paul and G. N. Patey, *J. Phys. Chem. B*, 2008, **112**, 11106–11111.
51 J. Mondal, G. Stirnemann and B. J. Berne, *J. Phys. Chem. B*, 2013, **117**, 8723–8732.
52 B. Hess, C. Kutzner, D. van der Spoel and E. Lindahl, *J. Chem. Theory Comput.*, 2008, **4**, 435–447.
53 S. Pronk, S. Pall, R. Schulz, P. Larsson, P. Bjelkmar, R. Apostolov, M. R. Shirts, J. C. Smith, P. M. Kasson, D. van der Spoel, B. Hess and E. Lindahl, *Bioinformatics*, 2013, **29**, 845–854.
54 W. L. Jorgensen, D. S. Maxwell and J. Tirado-Rives, *J. Am. Chem. Soc.*, 1996, **118**, 11225–11236.
55 H. J. C. Berendsen, J. R. Grigera and T. P. Straatsma, *J. Phys. Chem.*, 1987, **91**, 6269–6271.
56 S. Weerasinghe and P. E. Smith, *J. Phys. Chem. B*, 2003, **107**, 3891–3898.
57 L. Larini and J.-E. Shea, *J. Phys. Chem. B*, 2013, **117**, 13268–13277.
58 C. Hoelzel, P. Kibies, S. Imoto, R. Frach, S. Suladze, R. Winter, D. Marx, D. Horine and S. M. Kast, *J. Chem. Phys.*, 2016, **144**, 144104.
59 V. P. Voloshin, N. N. Medvedev, N. Smolin, A. Geiger and R. Winter, *J. Phys. Chem. B*, 2015, **119**, 1881–1890.
60 F. Rodriguez-Ropero, P. Rötzscher and N. F. A. van der Vegt, *J. Phys. Chem. B*, 2016, **120**, 8757–8767.
61 H. M. Berman, J. Westbrook, Z. Feng, G. Gilliland, T. N. Bhat, H. Weissig, I. N. Shindyalov and P. E. Bourne, *Nucleic Acids Res.*, 2000, **28**, 235–242.
62 N. Smolin and R. Winter, *J. Phys. Chem. B*, 2008, **112**, 997–1006.
63 T. Darden, D. York and L. Pedersen, *J. Chem. Phys.*, 1993, **98**, 10089–10092.
64 U. Essmann, L. Perera, M. L. Berkowitz, T. Darden, H. Lee and L. G. Pedersen, *J. Chem. Phys.*, 1995, **103**, 8577–8593.
65 S. Nosé and M. L. Klein, *Mol. Phys.*, 1983, **50**, 1055–1076.
66 M. Parrinello and A. Rahman, *J. Appl. Phys.*, 1981, **52**, 7182–7190.
67 G. Panick, G. J. A. Vidugiris, R. Malessa, G. Rapp, R. Winter and C. A. Royer, *Biochemistry*, 1999, **38**, 4157–4164.
68 G. Panick, R. Malessa, R. Winter, G. Rapp, K. J. Frye and C. Royer, *J. Mol. Biol.*, 1998, **275**, 389–402.
69 V. P. Voloshin, N. N. Medvedev, M. N. Andrews, R. R. Burri, R. Winter and A. Geiger, *J. Phys. Chem. B*, 2011, **115**, 14217–14228.
70 N. N. Medvedev, V. P. Voloshin, A. V. Kim, A. V. Anikeenko and A. Geiger, *J. Struct. Chem.*, 2013, **54**, 271–288.
71 V. Kim, V. P. Voloshin, N. N. Medvedev and A. Geiger, in *Transactions on Computational Science XX*, ed. M. L. Gavrilova, C. J. K. Tan and B. Kalantari, Springer, Berlin, Heidelberg, 2013, vol. 8110, pp. 56–71.
72 V. P. Voloshin, N. N. Medvedev and A. Geiger, in *Transactions on Computational Science XXII*, ed. M. L. Gavrilova and C. J. K. Tan, Springer, Berlin, Heidelberg, 2014, vol. 8360, pp. 156–172.
73 V. P. Voloshin, A. V. Kim, N. N. Medvedev, R. Winter and A. Geiger, *Biophys. Chem.*, 2014, **192**, 1–9.
74 A. V. Kim, N. N. Medvedev and A. Geiger, *J. Mol. Liq.*, 2014, **189**, 74–80.
75 V. P. Voloshin, N. N. Medvedev, N. Smolin, A. Geiger and R. Winter, *Phys. Chem. Chem. Phys.*, 2015, **17**, 8499–8508.
76 L. Mitra, N. Smolin, R. Ravindra, C. Royer and R. Winter, *Phys. Chem. Chem. Phys.*, 2006, **8**, 1249–1265.
77 I. Brovchenko, R. R. Burri, A. Krukau, A. Oleinikova and R. Winter, *J. Chem. Phys.*, 2008, **129**, 195101.
78 T. V. Chalikian, *Annu. Rev. Biophys. Biomol. Struct.*, 2003, **32**, 207–235.
79 D. Paschek, *J. Chem. Phys.*, 2004, **120**, 10605–10617.
80 A. K. Soper, E. W. Castner and A. Luzar, *Biophys. Chem.*, 2003, **105**, 649–666.
81 C. Hu, J. Rösgen and B. M. Pettitt, in *Modeling Solvent Environments*, ed. M. Feig, Wiley, 2010, pp. 77–92.
82 S. Funkner, M. Havenith and G. Schwaab, *J. Phys. Chem. B*, 2012, **11**, 13374–13380.

83 H. Lee, J. Choi, P. K. Verma and M. Cho, *J. Phys. Chem. A*, 2016, **120**, 5874–5886.
84 G. S. Jas, E. C. Rentchler, A. M. Slowicka, J. R. Hermansen, C. K. Johnson, C. R. Middaugh and K. Kuczera, *J. Phys. Chem. B*, 2016, **120**, 3089–3099.
85 A. V. Okhulkov, Yu. N. Demianets and Yu. E. Gorbaty, *J. Chem. Phys.*, 1993, **100**, 1578–1588.
86 D. Paschek, T. Engels, A. Geiger and W. von Rybinski, *Colloids Surf.*, 1999, **156**, 489–500.
87 D. Paschek, *J. Chem. Phys.*, 2004, **120**, 6674–6689.
88 P. Ganguly, T. Hajari, J. E. Shea and N. F. van der Vegt, *J. Phys. Chem. Lett.*, 2015, **6**, 581–585.
89 G. Anand, S. N. Jamadagni, S. Garde and G. Belfort, *Langmuir*, 2010, **26**, 9695–9702.
90 L. B. Sagle, K. Cimat, V. A. Litosh, Y. Liu, S. C. Flores, X. Chen, B. Yu and P. S. Cremer, *J. Am. Chem. Soc.*, 2011, **133**, 18707–18712.
91 T. Biben, P. Bladon and D. Frenkel, *J. Phys.: Condens. Matter*, 1996, **8**, 10799.
92 L. Sapir and D. Harries, *Curr. Opin. Colloid Interface Sci.*, 2015, **20**, 3–10.
93 L. Sapir and D. Harris, *J. Phys. Chem. Lett.*, 2014, **5**, 1061–1065.
94 S. Sukenik, L. Sapir and D. Harris, *Curr. Opin. Colloid Interface Sci.*, 2013, **18**, 495–501.